Astronomy & Astrophysics 451, 845-850 (2006) May 5, 2006
(DOI: 10.1051/0004-6361:20054790)

Radio Linear and Circular Polarization from M81*

Andreas Brunthaler[1,2], Geoffrey C. Bower[3], Heino Falcke[4,5]

[1] Joint Institute for VLBI in Europe, Postbus 2, 7990 AA Dwingeloo, The Netherlands
[2] Max-Planck-Institut für Radioastronomie, Auf dem Hügel 69, 53121 Bonn, Germany
[3] Radio Astronomy Laboratory, University of California, Berkeley, CA 94720, USA
[4] ASTRON, Postbus 2, 7990 AA Dwingeloo, The Netherlands
[5] Department of Astrophysics, Radboud Universiteit Nijmegen, Postbus 9010, 6500 GL Nijmegen, The Netherlands

Received 30 December 2005 / Accepted 19 January 2006

Abstract. We present results from archival Very Large Array (VLA) data and new VLA observations to investigate the long term behavior of the circular polarization of M81*, the nuclear radio source in the nearby galaxy M81. We also used the Berkeley-Illinois-Maryland Association (BIMA) array to observe M81* at 86 and 230 GHz. M81* is unpolarized in the linear sense at a frequency as high as 86 GHz and shows variable circular polarization at a frequency as high as 15 GHz. The spectrum of the fractional circular polarization is inverted in most of our observations. The sign of circular polarization is constant over frequency and time. The absence of linear polarization sets a lower limit to the accretion rate of $10^{-7} M_{\odot} y^{-1}$. The polarization properties are strikingly similar to the properties of Sgr A*, the central radio source in the Milky Way. This supports the hypothesis that M81* is a scaled up version of Sgr A*. On the other hand, the broad band total intensity spectrum declines towards milimeter wavelengths which differs from previous observations of M81* and also from Sgr A*.

Key words. galaxies: active, galaxies: individual: Messier Number: M81, polarization

1. Introduction

The nearby spiral galaxy M81 (NGC 3031) shares many properties with the Milky Way. It is similar in type, size and mass and it also contains a nuclear radio source, M81*, that is most likely associated with a supermassive black hole. M81* has been studied extensively using Very Long Baseline Interferometry (VLBI) in the past. Bietenholz, Bartel, & Rupen (2000) resolved M81* into a stationary core with a one sided jet. Multi-wavelength (Ho, Filippenko, & Sargent 1996) and sub-millimeter observations (Reuter & Lesch 1996) showed many similarities between M81* and Sgr A*, the central radio source in our Milky Way (Melia & Falcke 2001). A jet model of Sgr A* has been applied to M81*, where it can reproduce the radio flux density and the size of the radio core by changing the accretion rate (Falcke 1996). The sizes of both radio sources show a $\sim 1/\nu$ dependency on the frequency (e.g. Bietenholz, Bartel, & Rupen 2004 for M81*, and Bower et al. 2004 and Shen et al. 2005 for Sgr A*).

M81* is an apparent transitional object between Sgr A* and high luminosity AGN. As the brightest of the nearby low luminosity AGN (LLAGN), it is 5 orders of magnitude brighter than Sgr A* at radio wavelengths. M81* is substantially underluminous at X-ray wavelengths ($L \sim 10^{-5} L_{edd}$), yet not as much as Sgr A* ($L \sim 10^{-10} L_{edd}$). Still, it is the faintest LLAGN we can study.

Send offprint requests to: brunthal@mpifr-bonn.mpg.de

Furthermore, the polarization properties of M81* and Sgr A* are very similar. Sgr A* shows circular polarization in absence of linear polarization (Bower, Falcke, & Backer 1999, Bower et al. 1999a, 1999b) and we detected the same behaviour in M81* (Brunthaler et al. 2001.) The polarization properties of Sgr A* and M81* are in contrast to the properties of most radio jets in active galactic nuclei where linear polarization often exceeds circular polarization by a large factor (e.g. Wardle et al. 1998; Rayner, Norris, & Sault 2000). The absence of linear polarized emission in Sgr A* can be explained as a consequence of the accretion flow.

Bower et al. (2002) investigated the long term behavior of the circular polarization in Sgr A* from archival VLA data and showed that *i)* the circular polarization is variable on timescales of days to months, *ii)* the sign of the circular polarization stayed constant over the entire time range of almost 20 years, and *iii)* the average spectrum of circular polarization is inverted.

After the discovery of circular polarization in M81* we used the VLA to investigate the variability of the circular polarization on short timescales. We used additional archival VLA data to investigate the long term behavior of the circular polarization of M81*.

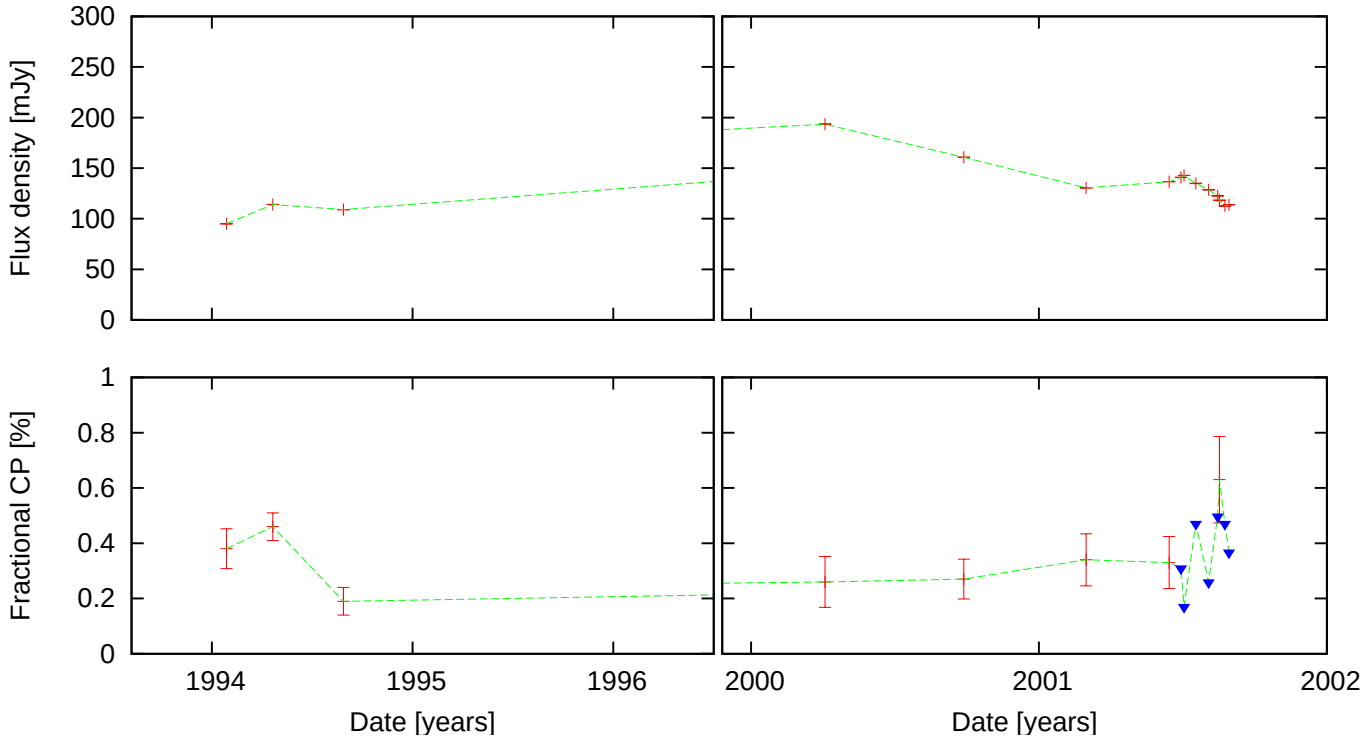

Fig. 1. Light-curve in total intensity (top) and fractional circular polarization of M81* at 4.8 GHz for the archival data (left) and the new observations (right). The filled triangles are 3σ upper limits. The two data points in 2000 are taken from Brunthaler et al. (2001)

2. Observations

2.1. Archival VLA Data

M81* and the supernova SN1993J in M81 were observed many times with the Very Long Baseline Array (VLBA) and the phased Very Large Array (VLA) over the last decade (e.g. Bartel et al. 1994; Bietenholz, Bartel, & Rupen 2000). The observations were typically 16 hours in duration, were made at different frequencies and involved rapid switching between M81*, SN1993J and scans roughly every hour on the extragalactic background source 0954+658 for calibration purposes. We used the VLA data from the observations on 5 November 1993 (ν = 8.4 and 15 GHz), 16 December 1993 (8.4 and 15 GHz), 29 January 1994 (4.8 and 8.4 GHz), 21 April 1994 (4.8 GHz), 29 August 1994 (4.8 and 8.4 GHz), 31 October 1994 (8.4 GHz), 23 December 1994 (8.4 GHz), and 7 April 1996 (8.4 GHz). The VLA data had 50 MHz of bandwidth in two sidebands in right (RCP) and left (LCP) circular polarization modes.

Data reduction was performed with the Astronomical Image Processing System (AIPS). 3C 48 was used as primary amplitude calibrator. Then amplitude and phase self-calibration was performed on 0954+658. This forces 0954+658 to have zero circular polarization. The amplitude calibration was transfered to M81* and SN1993J before we performed phase self-calibration on M81* and SN1993J. Finally, we mapped all three sources in Stokes I and V. Flux densities were determined by fitting an elliptical Gaussian component to the sources.

2.2. New VLA observations

In addition to the archival VLA data, we used the VLA to observe M81* on 02 March 2001 and 9 dates between 15 June and 30 August 2001. During the latter period, the minimum and maximum separations between observing dates were 2 and 15 days, respectively. The VLA was in B configuration for the first observation and C array for the remaining observations. Observations were made at 5.0, 8.4, 15 and 22 GHz with 50 MHz of bandwidth in two sidebands in RCP and LCP modes.

Each observation was between two and four hours in duration. Observing and analysis was performed with AIPS and followed the procedures outlined in Brunthaler et al. (2001). The extragalactic point source J1044+719 was used as a phase, amplitude and polarization calibrator as well as reference pointing source. The extragalactic point source J1053+704 was used to check for polarization calibration errors . 3C 286 was used as an absolute amplitude calibration source. Finally, we mapped all three sources in Stokes I, U, Q, and V. Flux densities were determined by fitting an elliptical Gaussian component to the sources.

We also used the VLA to observe M81* on 09 August 2003 at 15 GHz, 22 GHz, and 43 GHz in polarimetric mode. The VLA was in A configuration with a resolution of about 50 milliarcseconds at 43 GHz. The total integration time on M81* was 8, 48, and 52 minutes at 15, 22 and 43 GHz respectively and spread over a time range of 11 hours. Phase and amplitude calibration were performed using the nearby compact source, J1056+714. Phase self-calibration was also performed on M81* to eliminate the effects of atmospheric decorrelation.

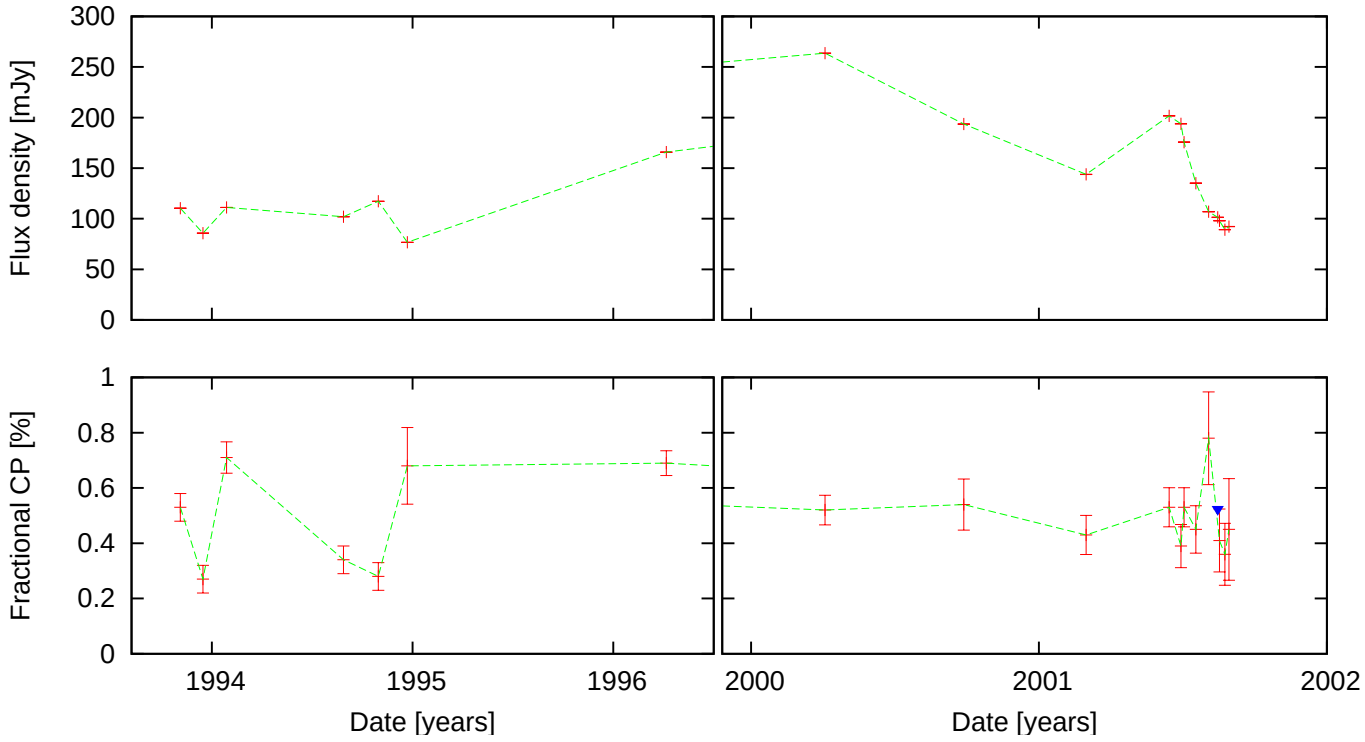

Fig. 2. Light-curve in total intensity (top) and fractional circular polarization of M81* at 8.4 GHz for the archival data (left) and the new observations (right). The filled triangle is an 3σ upper limit. The two data points in 2000 are taken from Brunthaler et al. (2001)

Polarization leakage calibration was performed using simultaneous full track observations of J1056+714 and J1048+701.

2.3. BIMA observations

We used the Berkeley-Illinois-Maryland Association (BIMA) array to observe M81* at 3 mm wavelength (Welch et al. 1996). Observations were made in the multiplexed polarimetric mode described in Bower et al. (1999b). The receivers were tuned to sky frequencies of 82.8 GHz (lower sideband) and 86.2 GHz (upper sideband). The compact source 0954+658 was used for phase calibration. Leakage calibration was determined from observations of 3C 279 on 11 November 2003. Observations of M81* were made on 6 dates in September and October 2003 (Table A.4). BIMA observations at 230 GHz on M81* were also performed in November 2003 (Table A.4). These data were also obtained in polarimetric mode with similar observing parameters to the 3 mm observations. Each observation was a 8 hour track.

2.4. Error Analysis

The Stokes parameter V is measured as the difference between the left- and right-handed parallel polarization correlated visibilities. Errors in circular polarization measurements with the VLA have numerous origins: thermal noise, gain errors, beam squint, second-order leakage corrections, unknown calibrator polarization, background noise and radio frequency interference. The errors caused by amplitude calibration errors, beam squint, and polarization leakage scale with the source strength, and therefore the fractional circular polarization is a more relevant indicator for the detection of circular polarization. A detailed discussion of these errors is given in Bower, Falcke, & Backer (1999) and Bower et al. (2002). We calculated the systematic errors based on the model for the VLA for circular polarization from Bower et al. (2002). For M81*, SN1993J, and J1053+704 the errors on the fractional circular polarization in Tables A.1 – A.3 are separated into statistical and systematic terms, while for the calibrator sources 0954+658 and J1044+719 only the statistical error is given. The calibrator sources do not have a systematic error, since their circular polarization was assumed to be zero during the calibration.

3. Results

3.1. Circular and Linear Polarization

The results for the archival data at 4.8, 8.4, and 15 GHz are shown in Tables A.1, A.2, and A.3 respectively. We consider circular polarization as detected if the measured flux density exceeds the combined statistical and systematic errors (added in quadrature) by a factor of three. 0954+658 showed no circular polarization as expected. M81* showed circular polarization in all observations except one (16 December 1993 at 15 GHz). SN1993J showed circular polarization only in one epoch (29 August 1994 at 4.8 GHz) and no circular polarization in all other observations. The upper limits on the circular polarization of SN1993J are not very meaningful at 15 GHz due to the low flux density and unexpected high noise.

The results for the new observations at 4.8, 8.4, and 15 GHz are shown in Tables A.1, A.2, and A.3 respectively. The

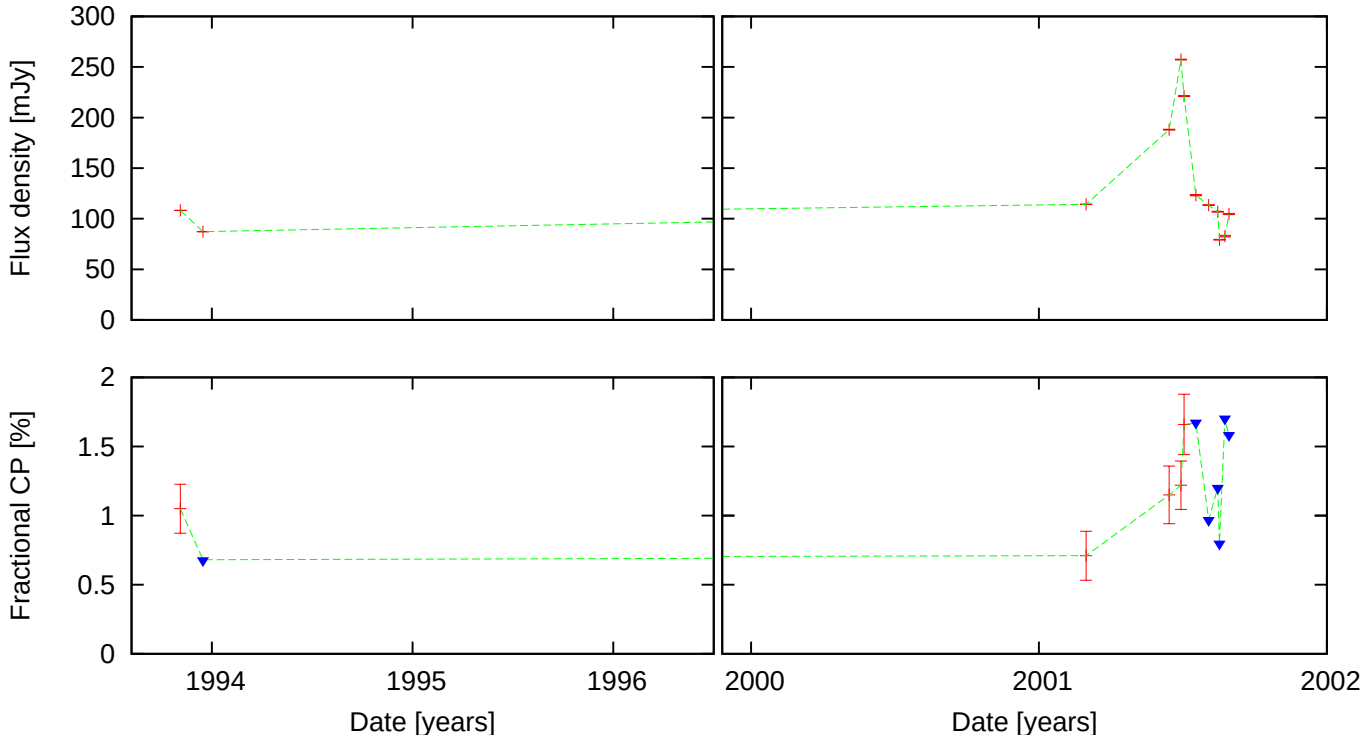

Fig. 3. Light-curve in total intensity (top) and fractional circular polarization of M81* at 15 GHz for the archival data (left) and the new observations (right). The filled triangles are 3σ upper limits.

22 GHz data and the high frequency observations on 9 August 2003 gave no useful limits on the circular polarization, mainly because the short integration time and higher systematic errors. At 4.8. 8.4, and 15 GHz, 1044+719 showed no circular polarization as expected. M81* showed circular polarization in three epochs at 4.8 GHz, all except one epoch at 8.4 GHz and four epochs at 15 GHz. The check source 1053+704 showed only circular polarization in two epochs at 15 GHz.

The three *detections* of circular polarization in the check sources SN1993J and 1053+704 are caused by either remaining amplitude calibration errors or by a small level of circular polarization in the sources. Since both sources show no circular polarization at 8.4 GHz, the frequency band with the highest sensitivity, it is most likely that the *detected* circular polarization in SN1993J and 1053+704 comes from residual amplitude calibration errors. The fractional circular polarization in M81* at 15 GHz is higher by a factor of 2 and 4 than in 1053+704 in the observations on 15 June 2001 and 4 July 2001 respectively. In these two cases, the measured circular polarization of M81* is probably only partly caused by the amplitude calibration errors.

In the BIMA observations at 86 and 230 GHz neither linear nor circular polarization is detected for M81* in any individual epoch. Mean linear polarization at 86 GHz is 1.2 mJy, or 1.6% (3σ). Mean circular polarization at 86 GHz is 2.8 ± 0.4 mJy, or 3.9 ± 0.5%. Although this is formally a detection, it is not clear whether systematic errors are significant. Due to the low flux density, limits on the polarized flux density are not significant at 230 GHz.

The 8.4 GHz data seems to be the most reliable data since M81* showed circular polarization in all epochs except one while the check sources SN1993J and 1053+704 never showed circular polarization. The light-curve of total intensity and fractional circular polarization is shown in Fig. 2. The fractional circular polarization shows significant variability on timescales of a few weeks which is not correlated with the variability in the total intensity. Between 4 August 2001 and 16 August 2001, the fractional circular polarization at 8.4 GHz dropped from 0.78% to less than 0.35% while the total intensity showed no significant change. However it is remarkable that, despite the strong variability, the sign of the circular polarization is always positive. At the other two frequencies, the sign is also positive when circular polarization is detected in M81*.

The spectrum of the fractional circular polarization is inverted ($\alpha > 0$ for $m_c \propto \nu^\alpha$) with values between 0.4 and 2 in most epochs when it was detected at more than one frequency. The mean spectral index between 4.8 and 8.4 GHz is 0.51, while the mean spectral index between 8.4 and 15 GHz is 1.52. Only the observation on 18 August 2001 shows a steep spectrum of α=-0.77 between 4.8 and 8.4 GHz..

Linear polarization was not detected in the VLA observations on 9 August 2003 and the BIMA observations at 86 GHz (Fig. 5). The archival data was not searched for linear polarization.

3.2. Total intensity

The high frequency VLA data taken on 9 August 2003 give a simultaneous total intensity spectrum of M81* that shows the

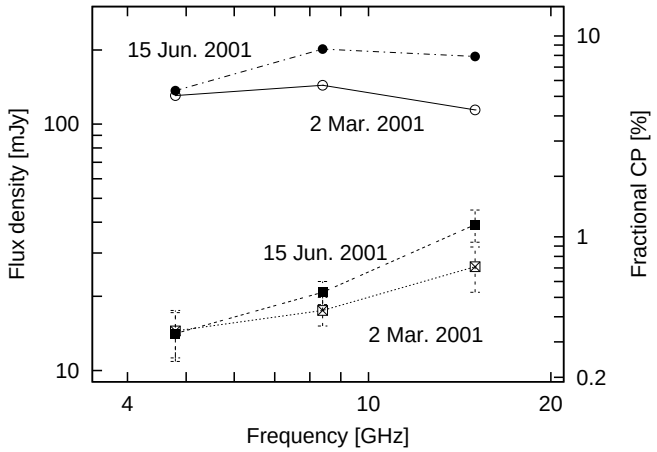

Fig. 4. Spectra of the total intensity (circles) and the fractional circular polarization (squares) from 2 March 2001 (open) and 15 June 2001 (filled).

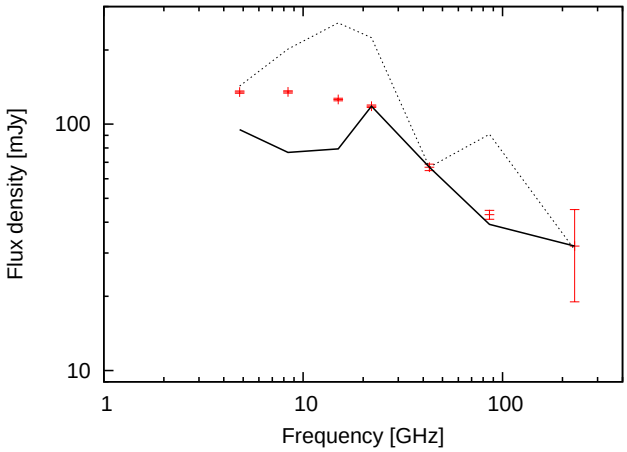

Fig. 6. Non simultaneous broad-band spectrum of M81*. Also shown are the maximal (dashed line) and minimal (solid line) measured values at each frequency.

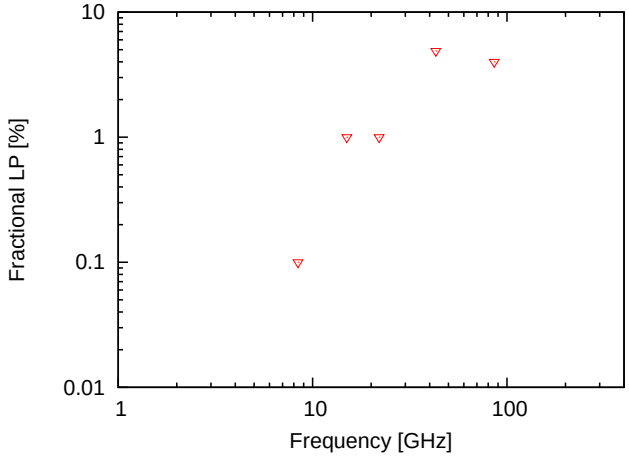

Fig. 5. 3 σ upper limits on the linear polarization of M81* up to 86 GHz. The 8.4 GHz data point is taken from Bower, Falcke, & Mellon (2002).

flux density decreasing from 15 to 43 GHz with a spectral index of ~ -0.6. In the BIMA observations M81* is clearly detected at 86 GHz in total intensity and is strongly variable on a time scale $\sim$ 10 days. The mean total intensity is 71 mJy. Due to low sensitivity, M81* is only marginally detected at 230 GHz in total intensity. The mean flux density for M81* from this observation is $31 \pm 4 \pm 15$ mJy, where the first error is the statistical error and the second error is the systematic error due to decorrelation. Atmospheric decorrelation may be serious and these results may significantly underestimate the total flux density of M81* (Table A.4).

Fig. 6 shows a non simultaneous broad-band spectrum of M81*. The 15 – 43 GHz data points are from the VLA observations on 9 August 2003. The 4.8 and 8.4 GHz data points are from the observation on 19 July 2001, where the 15 GHz flux was comparable to the 15 GHz flux in the 9 August 2003 observation. The 86 GHz and 230 GHz data points are from the BIMA observations on 7 September 2003 and November 2003 respectively. Also shown are the maximal and minimal measured values at each frequency in our observations. Although the spectrum is not simultaneous it is clear that the spectrum declines towards higher frequencies.

M81* underwent a flare in total intensity during the new VLA observations between June and August 2001. The peak was reached at 8.4 GHz before 15 June 2001, while the flux density continued to rise at 4.8 until 4 July 2001. At 15 GHz, the peak was reached in 30 June 2001. Fig. 7 shows the spectral indices between 4.8 and 8.4 GHz, and bewteen 8.4 and 15 GHz during this flare. The spectrum at the lower frequencies shows a smooth transition from an inverted ($\alpha \sim +0.7$) to a steep ($\alpha \sim -0.4$) spectrum. At higher frequencies, the spectral index does not follow a trend and is scattered between -0.4 and +0.5. The fast change in spectral index between 4.8 and 8.4 GHz could be caused by a drop in the turnover frequency of a syncrotron self-absorpted jet from above 8.4 to below 4.8 GHz and should be accompanied by a fast expansion of the jet. This behaviour is known in other active galactic nuclei (e.g. III Zw 2: Brunthaler et al. 2000, Brunthaler et al. 2005). The scatter of the spectral index between 8.4 and 15 GHz could be caused by multiple sub-flares that occur at 15 GHz.

4. Discussion

The origin of circular polarization in AGN is still not known. Several mechanisms have been proposed in the literature. Interstellar propagation effects predict a very steep spectrum (Macquart & Melrose 2000) which is not consistent with our observations. One possible mechanism could be Faraday conversion (Pacholczyk 1977; Jones & Odell 1977) of linear polarization to circular polarization caused by the lowest energy relativistic electrons. Bower, Falcke, & Backer (1999) proposed a simple model for Sgr A* in which low-energy electrons reduce linear polarization through Faraday de-polarization and convert linear polarization into circular polarization. Faraday conversion can also affect the spectral properties of circular polarization and may lead to a variety of spectral indices, including inverted spectra (Jones & Odell 1977). In inhomogeneous

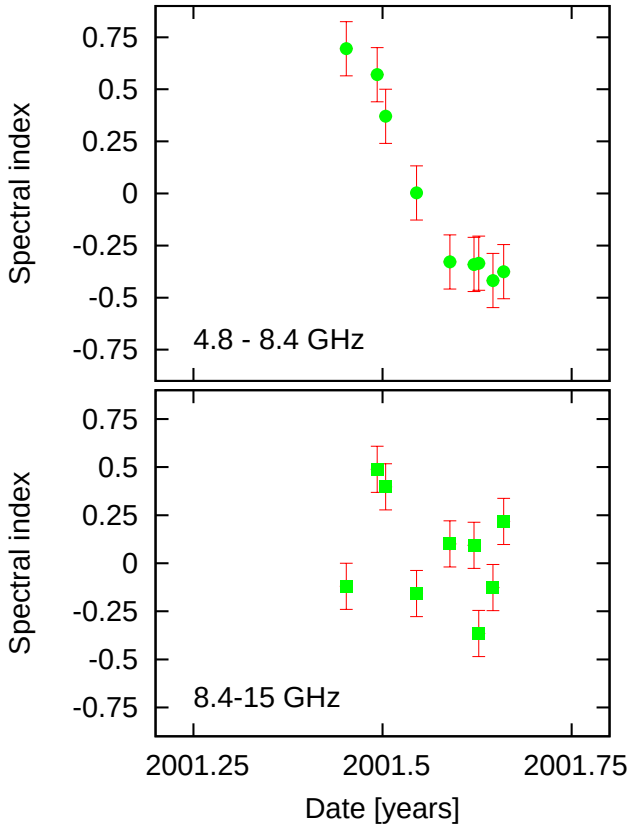

Fig. 7. Spectral indices of M81* between 4.8 and 8.4 GHz (top) and 8.4 and 15 GHz (bottom) during the flare in the new VLA observations.

sources, conversion can produce relatively high fractional circular polarization (Jones 1988). Gyro-synchrotron emission, can also lead to high circular polarization with an inverted spectrum and low linear polarization (Ramaty 1969). However, this mechanism is to some degree related and also requires that M81* and Sgr A* both contain a rather large number of low-energy electrons. Faraday conversion is also favored by Beckert & Falcke (2002) and Ruszkowski & Begelman (2002).

The long-term stability of the sign of circular polarization suggests that the Faraday conversion is connected to fundamental properties of the source and the material which is responsible for the conversion. It requires uniformity in the magnetic pole and accretion conditions over the observed timescales. One possible scenario is described by Enßlin (2003) where the sign of the circular polarization is connected to the sense of rotation of the central engine. In this scenario M81* is expected to rotate counter-clockwise.

The size of the radio emission of M81* at 8.4 GHz is ~ 0.45 mas, or ~ 1800 AU at 4 Mpc (Bietenholz et al. 1996). The fact that M81* is depolarized at at level of $< 0.1\%$ at the same frequency requires that the depolarizing material is also present at a scale of ~ 1800 AU.

While the polarization properties of M81* and Sgr A* are strikingly similar the total intensity spectrum seems to be different. In Sgr A*, the radio flux density rises towards the sub-mm regime (e.g. Zylka et al. 1995, Falcke & Markoff 2000). Our measurements indicate a different trend for M81*. Although the spectrum in Fig. 6 is not simultaneous and M81* shows strong variability our measured flux densities at 86 and 230 GHz are lower than the typical flux densities at centimeter wavelengths. This is different from the results in Reuter & Lesch (1996) who find an inverted spectrum up to ~ 100 GHz. We can not tell whether we observed M81* in a phase with unusual low millimeter emission or the Reuter & Lesch (1996) observations were made during an outburst at millimeter wavelengths. A simultaneous monitoring project from centimeter to millimeter wavelengths would be needed to decide this question.

Linear polarization is not detected for M81* at any wavelength longward of 3.6 mm. The presence of a jet at VLBI resolution, radio synchrotron emission, and circular polarization suggest that M81* is intrinsically linearly polarized but depolarized during propagation through a magnetized plasma. The case is similar to that of Sgr A*, which is detected in linear polarization only at wavelengths shortward of 3.6 mm. For Sgr A*, the detection of linear polarization at short wavelengths provides an upper limit to the rotation measure of a few times 10^6 rad m^{-2}. This provides an upper limit to the accretion rate of $\sim 10^{-7} M_\odot y^{-1}$. For M81*, we find a lower limit to the rotation measure of $\sim 10^4$ rad m^{-2} for the case of beam depolarization and $\sim 4\times10^5$ rad m^{-2} for the case of bandwidth depolarization, under the assumption that the intrinsic source is polarized. The lesser value could originate in the dense interstellar medium but the larger value exceeds that seen anywhere in the ISM. ADAF and Bondi-Hoyle accretion models will depolarize the source unless the accretion rate falls below $10^{-9} M_\odot y^{-1}$ (Quataert & Gruzinov 2000). However, for radiatively inefficient accretion flows, the larger of the RM limits implies a lower limit to the accretion rate of $10^{-7} M_\odot y^{-1}$. The accretion rate necessary for the X-ray luminosity is $10^{-5} M_\odot y^{-1}$. Since bandwidth depolarization effects decrease as λ^3, measurement of the linear polarization at a wavelength of 0.8 mm would increase the accuracy of the accretion rate constraint by nearly two orders of magnitude.

5. Summary & Conclusion

We have presented VLA observations of M81* from 1994 until 2002 that show that circular polarization is present at 4.8, 8.4, and 15 GHz in absence of linear polarization. The fractional circular polarization is variable on timescales of days and months and not correlated with the total flux density of the source. The sign of the circular polarization was, if detected, at all frequencies and times always positive. The polarization properties are strikingly similar to the properties of Sgr A*, the central radio source in the Milky Way. This supports the hypothesis that M81* is a scaled up version of Sgr A*. Aitken et al. (2000) and Bower et al. (2003) detected linear polarization at 230 GHz and higher frequencies that also shows variability (Bower et al. 2005; Marrone et al. 2006). Given the similarity between M81* and Sgr A* we expect to see also linear polarization in M81* at higher frequencies.

Acknowledgements. This research was partially supported by the DFG Priority Programme 1177. The National Radio Astronomy

Observatory is operated by Associated Universities, Inc., under a co-operative agreement with the National Science Foundation.

References

Aitken D. K., Greaves J., Chrysostomou A., et al., 2000, ApJ, 534, L173
Bartel N., Bietenholz M. F., Rupen M. P., et al., 1994, Nat., 368, 610
Beckert T., Falcke H., 2002, A&A, 388, 1106
Bietenholz M. F., Bartel N., Rupen M. P., 2000, ApJ, 532, 895
Bietenholz M. F., Bartel N., Rupen M. P., 2004, ApJ, 615, 173
Bietenholz M. F., Bartel N., Rupen M. P., et al., 1996, ApJ, 457, 604
Bower G. C., Backer D. C., Zhao J., Goss M., Falcke H., 1999a, ApJ, 521, 582
Bower G. C., Falcke H., Backer D. C., 1999, ApJ, 523, L29
Bower G. C., Falcke H., Herrnstein R. M., et al., 2004, Science, 304, 704
Bower G. C., Falcke H., Mellon R. R., 2002, ApJ, 578, L103
Bower G. C., Falcke H., Sault R. J., Backer D. C., 2002, ApJ, 571, 843
Bower G. C., Falcke H., Wright M. C., Backer D. C., 2005, ApJ, 618, L29
Bower G. C., Wright M. C. H., Backer D. C., Falcke H., 1999b, ApJ, 527, 851
Bower G. C., Wright M. C. H., Falcke H., Backer D. C., 2003, ApJ, 588, 331
Brunthaler A., Bower G. C., Falcke H., Mellon R. R., 2001, ApJ, 560, L123
Brunthaler A., Falcke H., Bower G. C., et al., 2000, A&A, 357, L45
Brunthaler A., Falcke H., Bower G. C., et al., 2005, A&A, 435, 497
Enßlin T. A., 2003, A&A, 401, 499
Falcke H., 1996, ApJ, 464, L67
Falcke H., Markoff S., 2000, A&A, 362, 113
Ho L. C., Filippenko A. V., Sargent W. L. W., 1996, ApJ, 462, 183
Jones T. W., 1988, ApJ, 332, 678
Jones T. W., Odell S. L., 1977, ApJ, 214, 522
Macquart J.-P., Melrose D. B., 2000, ApJ, 545, 798
Marrone D. P., Moran J. M., Zhao J.-H., Rao R., 2006, ApJ, 640, 308
Melia F., Falcke H., 2001, ARA&A, 39, 309
Pacholczyk A. G., 1977, Oxford Pergamon Press International Series on Natural Philosophy, 89
Quataert E., Gruzinov A., 2000, ApJ, 545, 842
Ramaty R., 1969, ApJ, 158, 753
Rayner D. P., Norris R. P., Sault R. J., 2000, MNRAS, 319, 484
Reuter H.-P., Lesch H., 1996, A&A, 310, L5
Ruszkowski M., Begelman M. C., 2002, ApJ, 573, 485
Shen Z.-Q., Lo K. Y., Liang M.-C., Ho P. T. P., Zhao J.-H., 2005, Nat., 438, 62
Wardle J. F. C., Homan D. C., Ojha R., Roberts D. H., 1998, Nat., 395, 457
Welch W. J., Thornton D. D., Plambeck R. L., et al., 1996, PASP, 108, 93
Zylka R., Mezger P. G., Ward-Thompson D., Duschl W. J., Lesch H., 1995, A&A, 297, 83

Appendix A: Tables

Table A.1. Circularly polarized flux at 4.8 GHz for M81* and calibrators. The errors on the fractional circular polarization are separated into statistical and systematic terms for the target and check source. For the calibrator source only the statistical error is given.

Date	Source	I [mJy]	P_c [mJy]	rms [mJy]	m_c [%]
28 Jan. 1994	0954+658	622.2	< 0.43	0.11	< 0.07 ± 0.02
	M81*	95.0	0.36	0.06	0.38 ± 0.06 ± 0.04
	SN1993J	77.1	< 0.17	0.05	< 0.22 ± 0.06 ± 0.03
21 Apr. 1994	0954+658	534.7	< 0.21	0.07	< 0.04 ± 0.01
	M81*	114.1	0.52	0.05	0.46 ± 0.04 ± 0.03
	SN1993J	62.1	< 0.22	0.04	< 0.35 ± 0.06 ± 0.03
29 Aug. 1994	0954+658	597.2	< 0.18	0.06	< 0.03 ± 0.01
	M81*	109.0	0.21	0.04	0.19 ± 0.04 ± 0.03
	SN1993J	54.6	0.18	0.03	0.33 ± 0.05 ± 0.03
02 Mar. 2001	1044+719	1568.2	0.11	0.11	< 0.01 ± 0.01
	M81*	130.5	0.44	0.10	0.34 ± 0.08 ±0.05
	1053+704	388.2	0.03	0.07	< 0.01 ± 0.02 ±0.06
15 Jun. 2001	1044+719	1710.9	0.33	0.35	< 0.02 ± 0.02
	M81*	136.7	0.45	0.11	0.33 ± 0.08 ±0.05
	1053+704	490.1	-0.58	0.21	< 0.12 ± 0.04 ±0.06
30 Jun. 2001	1044+719	1645.4	0.4	0.32	< 0.02 ± 0.02
	M81*	140.9	0.3	0.12	< 0.21 ± 0.09 ±0.05
	1053+704	497.5	-1.41	0.33	< 0.28 ± 0.07 ±0.07
04 Jul. 2001	1044+719	1687.5	0.01	0.01	< 0.01 ± 0.01
	M81*	142.8	0.12	0.05	< 0.09 ± 0.04 ±0.04
	1053+704	484	0.01	0.01	< 0.01 ± 0.01 ±0.05
19 Jul. 2001	1044+719	1645.3	0.08	0.24	< 0.01 ± 0.05
	M81*	134.9	0.46	0.19	< 0.34 ± 0.14 ±0.07
	1053+704	516.8	0.12	0.12	< 0.02 ± 0.02 ±0.10
04 Aug. 2001	1044+719	1641.8	0.1	0.31	< 0.01 ± 0.02
	M81*	128.6	0.07	0.07	< 0.05 ± 0.05 ±0.07
	1053+704	564.3	0.14	0.14	< 0.02 ± 0.02 ±0.10
16 Aug. 2001	1044+719	1636.5	0.06	0.23	< 0.01 ±0.01
	M81*	122.7	0.44	0.18	< 0.36 ± 0.15 ±0.07
	1053+704	524.3	-0.38	0.23	< 0.07 ±0.04 ±0.10
18 Aug. 2001	1044+719	1607.5	0.01	0.01	< 0.01 ± 0.01
	M81*	118.2	0.74	0.16	0.63 ± 0.14 ± 0.07
	1053+704	532.6	0.14	0.14	< 0.03 ± 0.03 ± 0.10
25 Aug. 2001	1044+719	1602.7	0.02	0.15	< 0.01 ± 0.01
	M81*	112.7	0.37	0.16	< 0.33 ± 0.14 ± 0.07
	1053+704	546	0.13	0.13	< 0.02 ± 0.02 ± 0.10
30 Aug. 2001	1044+719	1655.7	0.13	0.13	< 0.01 ± 0.01
	M81*	113.9	0.23	0.11	< 0.2 ± 0.10 ± 0.07
	1053+704	548	-0.08	0.14	< 0.01 ± 0.03 ± 0.10

Table A.2. Circularly polarized flux at 8.4 GHz for M81* and calibrators. The errors on the fractional circular polarization are separated into statistical and systematic terms for the target and check source. For the calibrator source only the statistical error is given.

Date	Source	I [mJy]	P_c [mJy]	rms [mJy]	m_c [%]
05 Nov. 1993	0954+658	663.5	< 0.27	0.04	< 0.04 ± 0.01
	M81*	110.4	0.59	0.03	0.53 ± 0.03 ± 0.04
	SN1993J	62.2	< 0.07	0.02	< 0.11 ± 0.03 ± 0.03
16 Dec. 1993	0954+658	655.5	< 0.12	0.04	< 0.02 ± 0.01
	M81*	85.7	0.23	0.03	0.27 ± 0.04 ± 0.03
	SN1993J	54.7	< 0.06	0.02	< 0.11 ± 0.04 ± 0.03
28 Jan. 1994	0954+658	600.6	< 0.24	0.08	< 0.04 ± 0.01
	M81*	111.2	0.79	0.04	0.71 ± 0.04 ± 0.04
	SN1993J	48.9	< 0.14	0.03	< 0.29 ± 0.06 ± 0.03
29 Aug. 1994	0954+658	648.1	< 0.11	0.04	< 0.02 ± 0.01
	M81*	102.0	0.35	0.03	0.34 ± 0.03 ± 0.04
	SN1993J	34.5	< 0.08	0.03	< 0.23 ± 0.09 ± 0.03
31 Oct. 1994	0954+658	670.9	< 0.12	0.04	< 0.02 ± 0.01
	M81*	117.2	0.33	0.03	0.28 ± 0.03 ± 0.04
	SN1993J	33.5	< 0.08	0.03	< 0.24 ± 0.09 ± 0.03
23 Dec. 1994	0954+658	693.7	< 0.43	0.14	< 0.06 ± 0.02
	M81*	76.7	0.52	0.09	0.68 ± 0.12 ± 0.07
	SN1993J	30.4	< 0.22	0.07	< 0.72 ± 0.23 ± 0.05
07 Apr. 1996	0954+658	786.3	< 0.11	0.04	< 0.01 ± 0.01
	M81*	165.8	1.15	0.03	0.69 ± 0.02 ± 0.04
	SN1993J	20.5	< 0.15	0.05	< 0.73 ± 0.24 ± 0.04
02 Mar. 2001	1044+719	1478.7	0.13	0.13	< 0.01 ± 0.01
	M81*	143.8	0.62	0.07	0.43 ± 0.05 ± 0.05
	1053+704	524.8	0.35	0.10	< 0.07 ± 0.02 ± 0.06
15 Jun. 2001	1044+719	2136.1	0.11	0.11	< 0.01 ± 0.01
	M81*	201.7	1.08	0.10	0.53 ± 0.05 ± 0.05
	1053+704	1006.1	0.17	0.17	< 0.02 ± 0.02 ± 0.06
30 Jun. 2001	1044+719	1488.6	0.01	0.01	< 0.01 ± 0.01
	M81*	193.9	0.75	0.11	0.39 ± 0.06 ± 0.05
	1053+704	763.0	0.34	0.19	< 0.04 ± 0.02 ± 0.07
04 Jul. 2001	1044+719	1525.8	0.57	0.57	< 0.04 ± 0.04
	M81*	175.7	0.93	0.09	0.53 ± 0.05 ± 0.05
	1053+704	753.3	0.13	0.13	< 0.02 ± 0.02 ± 0.06
19 Jul. 2001	1044+719	1474.8	0.10	0.10	< 0.01 ± 0.01
	M81*	135.1	0.60	0.09	0.45 ± 0.07 ± 0.05
	1053+704	769.2	0.27	0.13	< 0.04 ± 0.02 ± 0.07
04 Aug. 2001	1044+719	1485.4	0.12	0.12	< 0.01 ± 0.01
	M81*	107.0	0.84	0.17	0.78 ± 0.16 ± 0.05
	1053+704	785.1	0.57	0.26	< 0.07 ± 0.03 ± 0.07
16 Aug. 2001	1044+719	1469.1	0.27	0.27	< 0.02 ± 0.02
	M81*	101.4	0.36	0.16	< 0.35 ± 0.16 ± 0.07
	1053+704	758.3	1.20	0.27	< 0.16 ± 0.04 ± 0.10
18 Aug. 2001	1044+719	1476.8	0.41	0.65	< 0.03 ± 0.03
	M81*	98.0	0.40	0.09	0.41 ± 0.09 ± 0.07
	1053+704	775.2	0.41	0.30	< 0.05 ± 0.04 ± 0.10
25 Aug. 2001	1044+719	1406.9	0.11	0.11	< 0.01 ± 0.01
	M81*	89.2	0.32	0.09	0.36 ± 0.10 ± 0.05
	1053+704	746.0	1.30	0.24	< 0.17 ± 0.03 ± 0.07
30 Aug. 2001	1044+719	1520	0.17	0.17	< 0.01 ± 0.01
	M81*	92.3	0.42	0.16	0.45 ± 0.17 ± 0.07
	1053+704	789.2	0.30	0.30	< 0.04 ± 0.04 ± 0.10

Table A.3. Circularly polarized flux at 15 GHz for M81* and calibrators. The errors on the fractional circular polarization are separated into statistical and systematic terms for the target and check source. For the calibrator source only the statistical error is given.

Date	Source	I [mJy]	P_c [mJy]	rms [mJy]	m_c [%]
05 Nov. 1993	0954+658	664.5	< 0.26	0.09	< 0.04 ± 0.01
	M81*	108.2	1.14	0.18	1.05 ± 0.17 ± 0.05
	SN1993J	42.3	< 4.05	1.35	< 9.57 ± 3.19 ± 0.03
16 Dec. 1993	0954+658	606.4	< 0.28	0.09	< 0.05 ± 0.01
	M81*	87.2	< 0.06	0.19	< 0.07 ± 0.22 ± 0.05
	SN1993J	39.0	< 9.0	3.32	< 23.0 ± 8.51 ± 0.03
02 Mar. 2001	1044+719	999.8	0.03	0.12	< 0.01 ± 0.01
	M81*	114.2	0.81	0.19	0.71 ± 0.17 ± 0.05
	1053+704	485.2	0.25	0.18	< 0.05 ± 0.04 ± 0.07
15 Jun. 2001	1044+719	2275	0.36	0.36	< 0.02 ± 0.02
	M81*	188.1	2.16	0.38	1.15 ± 0.20 ± 0.06
	1053+704	1354.7	8.28	0.75	0.61 ± 0.06 ± 0.07
30 Jun. 2001	1044+719	1669.9	0.43	0.43	< 0.03 ± 0.03
	M81*	257.4	3.14	0.4	1.22 ± 0.16 ± 0.07
	1053+704	1051.5	2.61	0.66	< 0.25 ± 0.06 ± 0.09
04 Jul. 2001	1044+719	1955.8	1.67	1.67	< 0.09 ± 0.09
	M81*	221.2	3.66	0.46	1.66 ± 0.21 ± 0.06
	1053+704	1162.1	4.9	0.88	0.42 ± 0.08 ± 0.07
19 Jul. 2001	1044+719	1663.3	0.58	0.58	< 0.03 ± 0.03
	M81*	123.3	1.65	0.68	< 1.34 ± 0.55 ± 0.09
	1053+704	1011.9	1.76	1.05	< 0.17 ± 0.10 ± 0.12
04 Aug. 2001	1044+719	1663	0.29	1.14	< 0.02 ± 0.07
	M81*	113.4	0.36	0.36	< 0.31 ± 0.31 ± 0.09
	1053+704	973.4	6.42	1.92	< 0.66 ± 0.20 ± 0.12
16 Aug. 2001	1044+719	1876	0.51	0.51	< 0.03 ± 0.03
	M81*	107	0.38	0.42	< 0.35 ± 0.39 ± 0.09
	1053+704	1043.9	3.42	1.37	< 0.33 ± 0.13 ± 0.12
18 Aug. 2001	1044+719	1496.6	0.46	0.98	< 0.03 ± 0.07
	M81*	79.3	0.2	0.2	< 0.25 ± 0.25 ± 0.09
	1053+704	830.4	2.44	0.95	< 0.29 ± 0.11 ± 0.12
25 Aug. 2001	1044+719	1378	0.49	0.49	< 0.04 ± 0.04
	M81*	82.9	0.47	0.76	< 0.56 ± 0.56 ± 0.09
	1053+704	756.7	0.82	1.65	< 0.11 ± 0.22 ± 0.12
30 Aug. 2001	1044+719	1846.3	0.76	0.76	< 0.04 ± 0.04
	M81*	104.7	0.54	0.53	< 0.52 ± 0.52 ± 0.09
	1053+704	988.9	0.41	0.41	< 0.04 ± 0.04 ± 0.12

Table A.4. Polarized and total flux density of M81* at high frequencies unsing the VLA (15, 22, and 43 GHz) and BIMA (83, 86, and 230 GHz).

Date	Frequency [GHz]	Sideband	I [mJy]	Q [mJy]	U [mJy]	V [mJy]	m_p [%]
09 Aug. 2003	15		125.9 ± 1.5	< 1.4	< 1.4	< 1.4	< 1.0
	22		118.2 ± 1.3	< 1.1	< 1.1	< 1.3	< 1.0
	43		66.8 ± 2.0	< 3.3	< 3.3	< 4.2	< 4.9
07 Sep. 2003	83	lsb	44.0 ± 2.6	-2.0 ± 2.6	5.6 ± 2.6	0.3 ± 2.6	
	86	usb	41.8 ± 2.6	-1.8 ± 2.6	-3.4 ± 2.6	3.2 ± 2.6	
		avg	42.9 ± 1.8	-1.8 ± 1.8	1.1 ± 1.8	1.8 ± 1.8	5.1 ± 4.2
12 Sep. 2003	83	lsb	89.4 ± 1.8	-1.3 ± 1.8	-2.1 ± 1.8	5.7 ± 1.8	
	86	usb	92.4 ± 1.8	-0.8 ± 1.8	-1.1 ± 1.8	2.5 ± 1.8	
		avg	90.9 ± 1.3	-1.1 ± 1.3	-1.6 ± 1.3	4.1 ± 1.3	2.1 ± 1.4
21 Sep. 2003	83	lsb	86.4 ± 1.5	-0.2 ± 1.5	-0.7 ± 1.5	3.8 ± 1.5	
	86	usb	86.9 ± 1.5	-1.3 ± 1.5	-0.2 ± 1.5	3.4 ± 1.5	
		avg	86.7 ± 1.1	-0.2 ± 1.1	-0.5 ± 1.1	3.6 ± 1.1	0.6 ± 1.3
06 Oct. 2003	83	lsb	70.4 ± 2.0	3.5 ± 2.0	0.7 ± 2.0	0.2 ± 2.0	
	86	usb	72.7 ± 2.0	-0.3 ± 2.0	0.3 ± 2.0	3.5 ± 2.0	
		avg	71.6 ± 1.4	1.6 ± 1.4	0.5 ± 1.4	1.8 ± 1.4	2.3 ± 2.0
09 Oct. 2003	83	lsb	46.1 ± 1.8	5.1 ± 1.8	-2.1 ± 1.8	1.0 ± 1.8	
	86	usb	45.1 ± 1.8	-3.2 ± 1.8	2.7 ± 1.8	1.5 ± 1.8	
		avg	45.6 ± 1.3	1.0 ± 1.3	0.3 ± 1.3	1.2 ± 1.3	2.2 ± 2.9
12 Oct. 2003	83	lsb	43.9 ± 1.5	-2.4 ± 1.5	-1.0 ± 1.5	3.8 ± 1.5	
	86	usb	34.5 ± 1.5	6.1 ± 1.5	4.9 ± 1.5	-1.0 ± 1.5	
		avg	39.2 ± 1.1	1.9 ± 1.1	2.0 ± 1.1	1.4 ± 1.1	7.0 ± 2.8
01 Nov. 2003	230	lsb	33.7 ± 6	-6.6 ± 6	1.2 ± 6	-4.5 ± 6	
		usb	27.5 ± 6	2.7 ± 6	-19.9 ± 6	7.3 ± 6	
		avg	30.6 ± 4	-2.0 ± 4	-9.4 ± 4	1.4 ± 4	31.4 ± 13